Double fluorescent knock-in mice to investigate endogenous mu-delta opioid heteromer subscellular distribution.

Lyes Derouiche, Stéphane Ory, Dominique Massotte

1   **Title: Double fluorescent knock-in mice to investigate endogenous mu-delta opioid**
2   **heteromer subscellular distribution.**

3

4   Authors: Lyes Derouiche, Stéphane Ory and Dominique Massotte

5

6   Address:

7   Institut des Neurosciences Cellulaires et Intégratives, UPR 3212 CNRS, Strasbourg, France

8   Corresponding author:

9   Dominique Massotte

10   INCI UPR 3212 CNRS

11   5 rue Blaise Pascal

12   F-67084 Strasbourg cedex 03

13   France

14   Tel : +03 88 45 66 52

15   d.massotte@unistra.fr

16

17   Running title: Endogenous Mu-delta heteromer internalization

18

19   Key words: heteromers, opioid receptors, mu-delta, trafficking, primary neuronal culture,
20   GPCR

21

22   Number of words: 4943

23   Number of figures: 2

24   Number of tables: 1

25

ABSTRACT

The heteromerization of Mu (MOP) and delta (DOP) opioid receptors has been extensively

studied in heterologous systems. These studies demonstrated significant functional

interaction of MOP and DOP evidenced by new pharmacological properties and intracellular

signalling in transfected cells co-expressing the receptors. Due to the lack of appropriate

tools for receptor visualization, such as specific antibodies, the pharmacological and

functional properties of MOP-DOP heteromers in cells naturally expressing these receptors

remains poorly understood. To address endogenous MOP-DOP heteromer trafficking and

signalling in vivo and in primary neuronal cultures, we generated a double knock-in mouse

line expressing functional fluorescent versions of DOP and MOP receptors. This mouse

model has successfully been used to map the neuroanatomic distribution of the receptors

and to identify brain regions in which the MOP-DOP heteromers are expressed. Here, we

describe a method to quantitatively and automatically analyze changes in the subcellular

distribution of MOP-DOP heteromers in primary hippocampal culture from this mouse

model. This approach provides a unique tool to address specificities of endogenous MOP-

DOP heteromer trafficking.

INTRODUCTION

Opioid receptors belong to the subfamily of Class A G protein-coupled receptors (GPCRs).

Four subtypes of opioid receptors mu (MOP), delta (DOP), kappa (KOP) and nociceptin

(NOP) receptor respectively encoded by the *OPRM1*, *OPRD1*, *OPRK1* and *OPRL1* genes have

been identified several decades ago (for review see [1-3]). These seven transmembrane

domain receptors are functional in a monomeric form, but can also associate among

themselves to generate a larger assembly or with different subtypes of opioids or non-opioid

2

49   receptors. In the latter case, the new entity is called heteromer and may exhibit specific

50   functional properties.

51   In the case of the opioid system, MOP and DOP functional interactions are well documented

52   Among others, they are essential for the development of opiate tolerance [4,5]. Numerous

53   studies indicate that co-expression of the two receptors in heterologous systems promotes

54   the formation of MOP-DOP heteromers, which affects binding and signaling properties [6,7].

55   However, in spite of a growing body of evidence in favor of the presence of MOP-DOP

56   heteromers *in vivo*, the molecular mechanisms underlying functional interactions between

57   these two receptors remain poorly characterized[8]. This is mainly due to the lack of

58   appropriate tools, especially specific antibodies.

59   To deal with this issue and study MOP-DOP heteromers *in vivo*, we generated a double

60   fluorescent knock-in mouse line co-expressing DOP and MOP receptors respectively fused to

61   their C-terminus to the enhanced green fluorescent protein (DOP-eGFP) or mcherry (MOP-

62   mcherry). The DOP-eGFP and MOP-mCherry functional fusions allow highly specific and

63   simultaneous visualization of endogenously expressed receptors with subcellular resolution

64   and proved to be unique tools for neuroanatomical studies [9]. Mapping of MOP and DOP

65   receptors in the central and peripheral nervous systems indeed revealed MOP-DOP neuronal

66   co-expression in discrete neuronal networks essential for survival such as the nociceptive

67   pathway (see also mouse brain atlas at http://mordor.ics-mci.fr/). Specific targeting using the

68   fluorescent tags also revealed MOP-DOP physical proximity in the hippocampus providing

69   strong rationale for the existence of endogenous MOP-DOP heteromers [9]. In addition, the

70   double fluorescent knock-in mice represent unique tools to explore the dynamics of this

71   complex under physiological or pathological conditions and to characterize the functional

72   impact of MOP-DOP heteromers in the central and peripheral nervous system.

73   In this chapter, we describe optimized conditions for visualization of endogenous MOP-DOP

74   heteromers in primary hippocampal neurons obtained from the double fluorescent knock-in

75   mice. We also provide a protocol for automatic quantitative analysis of confocal images with

76   an open source software to determine changes in receptor subcellular localization. This

77   method allowed MOP-DOP heteromers monitoring and specific determination of their

78   intracellular fate upon pharmacological activation.

79   **MATERIAL AND METHODS**

80   **1. Animals**

81   Double knock-in mice co-expressing fluorescent DOP and MOP receptors were obtained by

82   crossing previously generated DOP-eGFP and MOP-mcherry knock-in mice. Briefly, DOP-

83   eGFP knock-in mice expressing the delta opioid receptor fused to its C-terminus to the eGFP

84   were generated by homologous recombination by inserting the eGFP cDNA into exon 3 of

85   the delta opioid receptor gene, in frame and 5′ from the stop codon [10]. MOP-mcherry

86   knock-in mice expressing the mu opioid receptor fused to its C-terminus to the red

87   fluorescent protein mCherry were generated by homologous recombination following a

88   procedure similar to the one used for DOR-eGFP knock-in mice [9]. The construct transfected

89   into ES cells comprised a Gly-Ser-Ile-Ala-Thr linker followed by the cDNA sequence

90   encoding the fluorescent protein (eGFP or mcherry). For subsequent clone selection, a

91   resistance gene was included that corresponded to neomycin flanked by loxP sites for DOP-

92   eGFP or to hygromycin flanked by FRT sites for MOP-mcherry (Figure 1). The resistance

93   gene was removed by microinjection of a plasmid expressing the recombinase. Blastocysts

94   were implanted in pseudo gestant BalbC females. Chimeric mice were crossed with C57Bl6/J

95   mice to obtain F1 heterozygous generation. Heterozygous animals were crossed to generate

96   mice homozygous for *Oprd1*-eGFP or *Oprm1*-mcherry that are fertile and develop normally.

97   Double knock-in animals were obtained by crossing the single knock-in mouse lines. The

98   genetic background of all mice was C57/BL6/J: 129svPas (50:50 %).

99   Mice were housed in animal facility under controlled temperature (21 ± 2 °C) and humidity

100   (45 ± 5 %) on a 12-h dark–light cycle with food and water ad libitum. All experiments were

101   performed in accordance to the European legislation (directive 2010/63/EU acting on

102   protection of laboratory animals) and the local ethical committee.

103   **2. Primary hippocampal culture**

104   **2.1. Material and reagents:**

105   • Double knock-in new born mice pups (P0-P3).

106   • 70% ethanol solution

107   • MilliQ water (autoclaved, or sterile filtered 0.22μm).

108   • Borate buffer *(see setup and procedures)*

109   • Poly-L-lysine hydrobromide (Sigma cat. No. P2623)

110   • 13 mm coverslips (Sigma, cat. no. P6407) coated with Poly-L-lysine *(see setup and*

111   *procedure)*

112   • 24-well sterile culture plates (Falcon cat. no. 353047).

113   • Pasteur pipets (flamed at the extremity, cotton plugged and autoclaved).

114   • Hibernate minus phenol red (BrainBits SKU: HAPR)

115   • Papain (Worthington, cat. no. LS003126)

116 • Dulbecco's Modified Eagle's Medium (DMEM) with 4.5g glucose (GIBCO, cat. no.

117 71966-029)

118 • Neurobasal A (GIBCO, cat. no. A13710-01)

119 • Foetal Calf Serum FCS heat inactivated. **Caution:** *test several batches to determine the*

120 *best one for your culture conditions.*

121 • Glutamax™ (GIBCO, cat. no. 35050061)

122 • L-glutamine (GIBCO, cat. no. 25030081)

123 • Penicillin-streptomycin (P/S) (cat. no. 15140122)

124 • DNAse (Sigma cat. no. DN25).

125 • B27 supplement (GIBCO, cat. no. 17504044)

126 • Trypan blue solution (Sigma, cat. no. T8154)

127 • Paraformaldehyde 32% solution diluted to 4% before use (*see setup and reagents*).

128 • Phosphate buffer saline (PBS). (Sigma-Aldrich, cat. no. P5493)

129 • Cell strainer 70μm (Falcon, cat. no. 352350)

130 **2.2. Setup and procedures**

131 **2.2.1. Borate buffer**: dissolve boric acid 1,24g and Sodium tetraborate (borax) 1,9g in 400ml

132 MilliQ H_2O. pH should be 8.4. Sterile filter (0.22μm) before use. **Caution:** *borax is a hazardous*

133 *substance, manipulate cautiously and eliminate waste according to the safety rules fixed by your*

134 *institution/government.*

135 **2.2.2. Coverslips sterilisation and coating**: put coverslips in a 100-mm petri dish, sterilise

136 in 70% ethanol during 2 h under gentle agitation, let dry completely under laminar flow, and

137 transfer to culture plates. Rinse once with MilliQ water. Coat coverslips with poly-L-lysine

138 25μg/ml final concentration in borate buffer; incubate at 37°C for 2h to overnight. Rinse 3

139 times with sterile water and pre-warm in DMEM medium. Coated coverslips may be

140 prepared several days before use, dried in the laminar flow hood and kept sealed at 4°C for

141 up to 1 month.

142 **2.2.3. Dissection medium**: Prepare 5 mL of of ice cold Hibernate supplemented with 1X P/S

143 and 0.5nM glutamax per animal and transfer 0.5 mL dissection medium in a 15-mL

144 centrifugation tube per animal (2 hippocampi).

145 **2.2.4. Enzyme solution**: prior to dissection, prepare a fresh solution of Papain at 40U/mL

146 concentration in Hibernate medium, incubate 5 minutes at 37°C in a water bath then keep on

147 ice until use. Prepare 0.5 mL per animal (2 hippocampi).

148 **2.2.5. Plating medium**: Prepare 12 mL DMEM medium supplemented with 4.5 g/l glucose

149 + 10% heat inactivated FCS + 2mM Glutamine + Pen/strep) per animal on the day of use.

150 **2.2.6. Growing medium**: Prepare 12 mL Neurobasal medium supplemented with 2% B27,

151 2mM glutamax, 0.5mM glutamine and 1X P/S per animal on the day of use.

152 **2.2.7. Phosphate-buffered saline (PBS):** prepare 1L 1X PBS working solution from 10X

153 stock solution by diluting with MilliQ water. Check the pH and adjust to 7.4 with 1M HCl or

154 1M NaOH solutions if needed. Sterile filter 0.22μm and keep at 4°C for up to 6 months.

155 **2.2.8. Fixation solution:** dilute paraformaldehyde (PFA) 32% solution to 4% final

156 concentration in PBS 0.1M, adjust pH to 7.4 if needed. Prepare 500μl per well for use in 24-

157 well plate. Keep up to 5 days at 4°C and up to 6 months at -20°C. ***Caution:*** *PFA a hazardous*

158 *highly toxic substance, manipulate under flow hood and eliminate waste according to the safety rules*

159 *fixed by your institution/government.*

160 **2.3. Dissection and culture procedures**

161 **2.3.1. Dissection and cell dissociation**

162 Decapitate pups. Transfer the head in a 33mm petri dish with 1.5 mL ice cold dissection

163 medium and isolate the brain. Place the isolated brain in a new 33mm petri dish with 1.5mL

164   ice cold dissection medium. Remove the meninges, dissect to isolate the two hippocampi and

165   keep them in 0.5mL dissection solution in a 15 mL-tube in ice. Add 0.5 mL of papain solution

166   per tube to 0.5 mL dissection medium (1mL final / 2 hippocampi). Place tubes in a water bath

167   at 37°C for 30 minutes with gentle shaking every 5-10 minutes. 5-10 minutes before digestion

168   ends, add DNase at a final concentration of 1mg/mL.

169   Remove papain solution by decantation, add 1mL of Hibernate, and triturate with Pasteur

170   pipet until the tissue is completely dissociated (about 15 to 20 times up-and-down are

171   sufficient) *(see note 1)*. Centrifuge at 1000g for 5 minutes at 22°C. Remove the supernatant,

172   add 1mL plating medium to resuspend cells (3 to 5 gentle up-and-down with Pasteur pipet).

173   Filter the cell suspension through a 70µm-cell strainer to remove any residual aggregates.

174   Count cells by diluting 20µl of cell suspension in 80µl of 1:10 Trypan blue solution diluted in

175   PBS. Place 20µl of this solution in a cell counting chamber and count cells excluding Trypan

176   blue (viable cells) only.

177   **2.3.2. Plating and feeding**

178   Prewarm poly-L-Lysine coated plates in DMEM medium at 37°C. Remove DMEM and plate

179   cells in 24-well plates at a density of 80 000 to 100 000 cells per well in a final volume of 500

180   µL.

181   Incubate in a humid incubator at 37°C and 5% CO2 and allow cells to adhere to the bottom of

182   plates during one hour. Remove the plating medium by aspiration, rinse once with 500µl of

183   prewarmed Neurobasal A medium, then add 500µl of growing medium and return back to

184   the incubator. Let cells grow during at least twelve days with half of the medium replaced

185   every four to five days.

186   **3. Processing and pharmacological treatments**

187   Pharmacological treatments should be realized between DIV 12 and DIV 15 after plating (*see*

188   *note 2)*. Ligands are added in a volume not exceeding 10% of the culture medium volume.

189   Incubate cells during the appropriate time. At the end of the pharmacological treatment,

190   remove the plate from the incubator and immediately place on ice, carefully aspirate the

191   medium and wash twice with ice cold sterile filtered PBS. Remove PBS and add 500µL of

192   PFA 4% in ice cold PBS and incubate during 20 minutes on ice. Remove PFA and rinse twice

193   with ice cold PBS and proceed to immunostaining or keep sealed with Parafilm in 500µL PBS

194   at 4°C up to 30 days *(see note 3).*

195   **4.   Immunocytofluorescence (ICF):**

196   **4.1.   Material and reagents**

197   • Phosphate buffer Saline 0.1M, pH 7.4.

198   • Normal Goat Serum (NGS) (Sigma cat. no. S26)

199   • Tween20 (Euromedex cat. no. 2001-B)

200   • Primary and secondary antibodies (see table 1)

201   • ProLong™ Gold Antifade Mounting medium (Molecular Probes cat. no. P36935).

202   • DAPI (Sigma cat. no. D9542)

203   • Finepoint Forceps (Rubis Switzerland cat.no.1K920)

204   • Microscope glass slides.

205   **4.2.   Setup and reagents**

206   4.2.1.   **PBS Tween 20 solution (PBST):** add 0.2% (V:V) of Tween 20 solution to 1X PBS

207   solution (*see section 1.2.7*) , mix vigorously to complete dissolution and keep at 4°C. Bring at

208   room temperature before use.

209   4.2.2.   **Blocking solution:** add 5% of Normal Goat Serum (NGS) to the PBST solution.

210   Prepare the day of use.

211   **4.3.   Method**

212   Incubate fixed cells in 250 μL of blocking solution for one hour under gentle agitation at

213   room temperature (20-22°C). Then remove the blocking solution by aspiration and incubate

214   2h at RT or overnight at 4°C with primary antibodies in blocking solution (250μL/well)

215   under gentle agitation. Wash three times in PBST and incubate for two hours protected from

216   light with specific secondary antibodies diluted in blocking solution (Table 1) (250μL/well).

217   Wash three times in PBST, incubate 5 minutes in DAPI solution (1μg/mL in PBS) for nuclei

218   staining and then wash three times in PBS followed by 1 wash in MilliQ H_2O. Remove

219   coverslips from wells with finepoint Forceps, let coverslips dry completely at room

220   temperature protected from light and mount on glass slides with ProLong™ Gold Antifade

221   mounting medium. Keep for up to one year at -20° protected from light.

222   **5.   Confocal microscope**

223   Images were acquired with a laser-scanning confocal microscope Leica SP5 using 63X /NA

224   1.4 oil immersion lens and X5 numerical zoom. The Pinhole was adjusted to 1 airy Unit and

225   the gain was adjusted without offset for each filter on a specific scanning plan allowing

226   specific acquisition without saturation. Image acquisition was performed according to

227   Nyquist parameters in XY with an average frame of 3 in a sequential scan mode to avoid

228   cross talk between different wavelengths. Z-stacks were obtained by scanning the whole

229   neuron thickness with step of 1 μm in z.

230   **6.   Image analysis with ICY open source software**

231 Confocal images were analyzed with ICY software (http://icy.bioimageanalysis.org/).

232 Quantification was performed on a single plane extracted from a z-stack. The analysis

233 combined two sequential steps. The first one consists in isolating each neuron to define

234 regions of interest (ROI). The second one involves the detection of the spots in each channel

235 and the determination of the amount of co-localisation in each ROI.

6.1.   ROI definition

237 Each neuron was carefully delineated using the "free-hand area" tool. This initial ROI is

238 filled with the "fill holes in ROI" plugin to define the total cell area (ROI $_{total}$). ROIs were then

239 processed to generate two ROIs corresponding to the cell periphery and the cytoplasm

240 (detailed protocol available online *http://icy.bioimageanalysis.org/*). Based on staining in basal

241 conditions, we estimated that most of the plasma membrane staining was found over an 8

242 pixels thickness. Therefore, we automatically eroded with the "Erode ROI" plugin the ROI

243 $_{total}$ by 8 pixels and subtracted this new ROI (ROI $_{cyto}$) to ROI $_{total}$ to obtain a ROI

244 corresponding to the cell periphery (ROI $_{peri}$).

6.2.   Spots detection and co-localisation

246 To detect specific signal in each ROI, we used the "spot detector" plugin which rely on the

247 wavelet transform algorithm [11]. By carefully setting the sensitivity threshold and the scale

248 of objects to detect, it allows detection of spots even in images with low signal to noise ratio.

249 In our conditions, the sensitivity threshold was fixed between 50 and 60 % and the scale of

250 objects set at 2 (pixel size 3) for mu and delta receptors. Once parameters were defined,

251 images were images were processed with the tool "protocol" in Icy which is a graphical

252 interface for automated image processing. Data including the number of spots detected in

253 each channel and ROIs, the number of co-localized objects and the ROI area were

254   automatically collected in excel files. Objects were considered co-localized if the distance of

255   their centroid was equal to or less than 3 pixels. The protocol is available online

256   (*NewColocalizer with binary and excel output v1_batch.xml*). To obtain histograms we calculated

257   object densities for each receptor reported to the surface of each ROI. Membrane to

258   cytoplasm density ratios were calculated to illustrate the subcellular distribution of each

259   receptor. The extend of co-localisation was calculated according to the following formula for

260   each ROI [$\% \ colocalisation = 100X \ (\frac{colocalised \ MOP \ and \ DOP \ objects}{\sum (\ detected \ MOP \ and \ DOP \ objects)})$].

261   **7. Statistical analysis**

262   Statistical analyses were performed with Graphpad Prism V7 software (GraphPad, San

263   Diego, CA). Normality of the distributions and homogeneity of the variances were checked

264   before statistical comparison to determine appropriate statistical analysis. In our case, data

265   were not normally distributed and the non-parametric Mann Witney test was used to

266   compare receptor densities in the plasma membrane and cytoplasm in basal conditions or

267   after agonist treatment. The extend of receptor co-localisation was compared using two-way

268   ANOVA with repeated measures followed by post-hoc Sidak's test for multiple

269   comparisons. Basal group was compared to agonist treated group (first factor) within

270   cytoplasm and plasma membrane localisation (second factor).

271   **RESULTS AND DISCUSSION**

272   In this chapter, we have presented an optimized method for monitoring the subcellular

273   distribution of endogenous MOP and DOP receptors. To this aim, we combined the use of a

274   genetically modified mouse line co-expressing functional fluorescently tagged receptors,

275   optimized primary neuronal culture protocol and automatic quantitative analysis of confocal

276   images with an open source software. Importantly, the image analysis procedure can be

277   easily implemented in any laboratory since data processing does not require extensive

278   mathematical developments or program writing with specialized software.

279   **Individual distribution of MOP and DOP receptors**

280   High magnification confocal images analyzed as single focal plan revealed discontinuous

281   and punctate distributions for DOP-eGFP and MOP-mCherry that were predominantly

282   located at the cell surface in basal conditions (Figure 2-A). Images also revealed a perinuclear

283   cytoplasmic localization of both receptors that likely correspond to receptor stock in the

284   endoplasmic reticulum. These observations were consistent with data from the literature

285   describing a predominant and membrane localization of DOP [10,12] and MOP [13] but also

286   substantial localization in perikarya [10].

287   Quantification using the ICY software indicated a higher density of fluorescent objects at the

288   cell surface for both MOP and DOP receptors (Figure 2-B) that was three times higher

289   compared to the cytoplasm (Fig. 2-C). Activation by the MOP-DOP agonist CYM51010 let to

290   the appearance of high intensity punctate structures in the cytoplasmic and a dramatic

291   decrease in the plasma membrane labelling of both receptors (figure 2-A). Accordingly, the

292   ratio corresponding to the density of fluorescent objects density at the plasma membrane

293   compared to the cytoplasm dropped dramatically from 3 to 1 for both MOP and DOP

294   receptors which supports internalization of the two receptors in vesicle-like structures.

295   These results are in agreement with previous reports using the density of fluorescence to

296   estimate changes in DOPeGFP subcellular distribution *in vivo*. In these studies, the ratio of

297   fluorescence density between the plasma membrane and cytoplasm was about 1.5 in basal

298   conditions and significantly decreased following agonist stimulation [10,14]. We therefore

299   tested our quantification method using images of DOR-eGFP neurons in the hippocampus

300   acquired with similar parameters in confocal microscopy. Using the protocol described

301   above, we found that the density in DOP-eGFP objects under basal conditions was around 3

302   similar to our results in primary neuronal cultures. We also established that this value

303   corresponded to a ratio in fluorescence density between the plasma membrane and the

304   cytoplasm of about 1.7, similar to previously reported ratios [10]. Moreover, we quantified

305   the ratio of fluorescence density between the plasma membrane and the cytoplasm using the

306   set of images used in Erbs et al 2016, and calculated a similar increase of about 10% in DOP-

307   eGFP expression at the plasma membrane after chronic morphine treatment in the neurons

308   of the hippocampus [15]. Altogether, these results fully validate the quantification method

309   developed using ICY software.

310   **Co-localization of MOP and DOP receptors and detection of MOP-DOP**

311   **heteromers**

312   Our analysis revealed substantial colocalization of MOP and DOP associated signals under

313   basal conditions. In fact, more than 22% of the MOP and DOP objects were co-localized

314   within the plasma membrane whereas cytoplasmic colocalization was fairly low (around

315   10%) (Figure 2-D). After selective MOP-DOP activation with the agonist CYM51010, the

316   cytoplasmic colocalization was increased by 87% to reach 18.7%. A two-fold decrease in the

317   percentage of MOP-DOP colocalization within the plasma membrane was also observed

318   after CYM51010 treatment (Figure 2-D). These observations support a view in which MOP

319   and DOP receptors remain associated upon specific activation of the heteromers and

320   undergo common intracellular fate.

321   It is however important to note, that due to the resolution limit of confocal microscopy,

322   MOP-DOP physical interaction has to be assessed by other experimental approaches such as

323   co-localization in electron microscopy or disruption of the physical contact by a

324   transmembrane peptide. The latter has been successfully performed for MOP-DOP receptors

325   *in vivo*. Indeed, a peptide corresponding to the MOP TM 1 or to the DOP second intracellular

326   loop in fusion with the cell transduction domain of the human immunodeficiency virus

327   (HIV) TAT protein interfered with MOP-DOP co-immunoprecipitation [16-18]. The recently

328   described proximity ligation assay [19] provides high spatial resolution and represents

329   another attractive option to address physical proximity.

330   In addition, the resolution of the images did not enable to distinguish the pool of receptors

331   associated to the plasma membrane from receptors located in the sub-membrane

332   compartment which represents another limitation of our analysis. Total internal reflection

333   fluorescence microscopy (TIRFM) would be required to differentiate the two compartments

334   and precisely monitor the first steps in receptor internalization.

335   MOPmcherry-DOPeGFP co-localisation studies could also be combined with identification of

336   the intracellular compartments using specific antibodies. This would enable for fine mapping

337   of the receptors in the vesicular structures and cellular compartments and would provide

338   detailed information on the intracellular fate of MOP-DOP heteromers.

339   **CONCLUSION**

340   Double knock-in mice represent unique tools to investigate endogenous MOP-DOP

341   neuroanatomical distribution but also to explore functional dynamics in physio-pathological

342   conditions. As described here, the use of double fluorescent knock-in mice combined with

confercal imaging and ICY software analyses enables easy quantification of receptor sub-

cellular distribution and co-localisation, hence specific MOP-DOP trafficking. Importantly,

the field of application of the method described here is not restricted to the study of MOP-

DOP heteromers but can be applied to address the heteromerization of any other pair of

GPCRs. Moreover, the analysis with the ICY software is not restricted to the study of

receptors but is widely applicable to monitor the co-localisation of any two objects detected

independently and can be applied to any type of high-resolution images.

NOTES

1- Cell dissociation is a critical step; if the trituration is too gentle, the tissue will not
   dissociate, if too vigorous cells will break.

2- Because re-expression of DOP-eGFP and MOP-mCherry is only detectable from day
   in vitro (DIV) 10 in primary neurons, pharmacological treatments should be
   performed between DIV12 and DIV15 to ensure full expression of the receptors.

3- Paraformaldehyde fixation decreases the fluorescence intensity of eGFP and mCherry
   and amplification by immunostaining is recommended. The DOP-eGFP construct can
   also be used for *ex vivo* real-time imaging of receptor internalization by confocal
   microscopy [10]. However, due to the low expression level of endogenous MOP
   receptors and their weak expression at the plasma membrane in basal conditions,
   real-time monitoring of MOP-mcherry remains presently below the detection limit.

ACKNOWLEDGMENTS

366 CONFLICT OF INTEREST

367 The authors declare no conflict of interest

368 REFERENCES

369   1. Charbogne P, Kieffer BL, Befort K (2014) 15 years of genetic approaches in vivo for

370 addiction research: Opioid receptor and peptide gene knockout in mouse models of drug

371 abuse. Neuropharmacology 76 Pt B:204-217. doi:10.1016/j.neuropharm.2013.08.028

372   2. Pasternak GW (2014) Opioids and their receptors: Are we there yet?

373 Neuropharmacology 76 Pt B:198-203. doi:10.1016/j.neuropharm.2013.03.039

374   3. Civelli O (2008) The orphanin FQ/nociceptin (OFQ/N) system. Results Probl Cell

375 Differ 46:1-25. doi:10.1007/400_2007_057

376   4. Ong EW, Cahill CM (2014) Molecular Perspectives for mu/delta Opioid Receptor

377 Heteromers as Distinct, Functional Receptors. Cells 3 (1):152-179. doi:10.3390/cells3010152

378   5. Gendron L, Mittal N, Beaudry H, Walwyn W (2015) Recent advances on the delta

379 opioid receptor: from trafficking to function. Br J Pharmacol 172 (2):403-419.

380 doi:10.1111/bph.12706

381   6. Gomes I, Ijzerman AP, Ye K, Maillet EL, Devi LA (2011) G protein-coupled receptor

382 heteromerization: a role in allosteric modulation of ligand binding. Mol Pharmacol 79

383 (6):1044-1052. doi:10.1124/mol.110.070847

384   7. Fujita W, Gomes I, Devi LA (2014) Revolution in GPCR signalling: opioid receptor

385   heteromers as novel therapeutic targets: IUPHAR review 10. Br J Pharmacol 171 (18):4155-

386   4176. doi:10.1111/bph.12798

387   8. Massotte D (2015) In vivo opioid receptor heteromerization: where do we stand? Br J

388   Pharmacol 172 (2):420-434. doi:10.1111/bph.12702

389   9. Erbs E, Faget L, Scherrer G, Matifas A, Filliol D, Vonesch JL, Koch M, Kessler P,

390   Hentsch D, Birling MC, Koutsourakis M, Vasseur L, Veinante P, Kieffer BL, Massotte D

391   (2015) A mu-delta opioid receptor brain atlas reveals neuronal co-occurrence in subcortical

392   networks. Brain Struct Funct 220 (2):677-702. doi:10.1007/s00429-014-0717-9

393   10. Scherrer G, Tryoen-Toth P, Filliol D, Matifas A, Laustriat D, Cao YQ, Basbaum AI,

394   Dierich A, Vonesh JL, Gaveriaux-Ruff C, Kieffer BL (2006) Knockin mice expressing

395   fluorescent delta-opioid receptors uncover G protein-coupled receptor dynamics in vivo.

396   Proc Natl Acad Sci U S A 103 (25):9691-9696. doi:10.1073/pnas.0603359103

397   11. Olivo-Marin JC (2002) Extraction of spots in biological images using multiscale

398   products. Pattern Recogn 35 (9):1989-1996. doi:Pii S0031-3202(01)00127-3 Doi 10.1016/S0031-

399   3203(01)00127-3

400   12. Cahill CM, McClellan KA, Morinville A, Hoffert C, Hubatsch D, O'Donnell D,

401   Beaudet A (2001) Immunohistochemical distribution of delta opioid receptors in the rat

402   central nervous system: evidence for somatodendritic labeling and antigen-specific cellular

403   compartmentalization. J Comp Neurol 440 (1):65-84

404   13. Trafton JA, Abbadie C, Marek K, Basbaum AI (2000) Postsynaptic signaling via the

405   [mu]-opioid receptor: responses of dorsal horn neurons to exogenous opioids and noxious

406   stimulation. J Neurosci 20 (23):8578-8584

407   14. Faget L, Erbs E, Le Merrer J, Scherrer G, Matifas A, Benturquia N, Noble F,

408   Decossas M, Koch M, Kessler P, Vonesch JL, Schwab Y, Kieffer BL, Massotte D (2012) In vivo

409   visualization of delta opioid receptors upon physiological activation uncovers a distinct

410   internalization profile. J Neurosci 32 (21):7301-7310. doi:10.1523/JNEUROSCI.0185-12.2012

411   15. Erbs E, Faget L, Ceredig RA, Matifas A, Vonesch JL, Kieffer BL, Massotte D (2016)

412   Impact of chronic morphine on delta opioid receptor-expressing neurons in the mouse

413   hippocampus. Neuroscience 313:46-56. doi:10.1016/j.neuroscience.2015.10.022

414   16. He SQ, Zhang ZN, Guan JS, Liu HR, Zhao B, Wang HB, Li Q, Yang H, Luo J, Li ZY,

415   Wang Q, Lu YJ, Bao L, Zhang X (2011) Facilitation of mu-opioid receptor activity by

416   preventing delta-opioid receptor-mediated codegradation. Neuron 69 (1):120-131.

417   doi:10.1016/j.neuron.2010.12.001

418   17. Kabli N, Martin N, Fan T, Nguyen T, Hasbi A, Balboni G, O'Dowd BF, George SR

419   (2010) Agonists at the delta-opioid receptor modify the binding of micro-receptor agonists to

420   the micro-delta receptor hetero-oligomer. Br J Pharmacol 161 (5):1122-1136.

421   doi:10.1111/j.1476-5381.2010.00944.x

422   18. Xie WY, He Y, Yang YR, Li YF, Kang K, Xing BM, Wang Y (2009) Disruption of

423   Cdk5-associated phosphorylation of residue threonine-161 of the delta-opioid receptor:

424   impaired receptor function and attenuated morphine antinociceptive tolerance. J Neurosci 29

425   (11):3551-3564. doi:10.1523/JNEUROSCI.0415-09.2009

426   19. Dasiel O. Borroto-Escuela BH, Miles Woolfenden , Luca Pinton , Antonio Jiménez-

427   Beristain , Julia Ofl ijan , Manuel Narvaez , Michael Di Palma , Kristin Feltmann , Stfano

428   Sartini , Patrizia Ambrogini , Francisco Ciruela , Riccardo Cuppini , and Kjell Fuxe (2016) In

429   Situ Proximity Ligation Assay to Study and Understand the Distribution and Balance of

430 GPCR Homo- and Heteroreceptor Complexes in the Brain. Neuromethods, vol 110 Springer

431 Science+Business Media New York edn. doi:DOI 10.1007/978-1-4939-3064-7_9

432

433 **TABLE 1: Primary and secondary antibodies**

Antigen	Antibody	Supplier reference	Dilution
eGFP	Chicken IgY	AVES-GFP1020	1/1000
mCherry	Rabbit IgG	Clontech-632496	1/1000
Chicken IgY	Goat anti chicken Alexa Fluor 488	Molecular Probes-A11039	1/2000
Rabbit IgG	Goat anti rabbit Alexa Fluor 594	Molecular Probes-A11012	1/2000

434

435 **FIGURE LEGENDS**

436 **Figure 1: Double Knock-in DOP-eGFP/MOP-mCherry mouse engineering**. **A)**

437 Construction of the DOP-eGFP mouse. A cDNA sequence corresponding to the eGFP cDNA,

438 and the FRT flanked neomycine (neo) cassette was inserted by homologous recombination

439 (HR) into the *Oprd1* locus. HR was followed Cre recombinase treatment in ES cells. **B)**

440 Construction of the MOP-mcherry mouse. A cDNA sequence corresponding mCherry

441 cDNA, and the loxP flanked hygromycine (hygro) cassette were inserted by HR to the *Oprm1*

442 locus. HR was followed by FRT recombinase treatment in ES cells. **(C)** Double knock-in mice

443 were obtained by crossing homozygote DOP-eGFP and MOP-mCherry mice.

444 **Figure 2: MOP-DOP heteromer visualisation and quantification**. **A)** Representative

445 confocal images illustrating MOP-mcherry and DOP-eGFP co-localisation in basal conditions
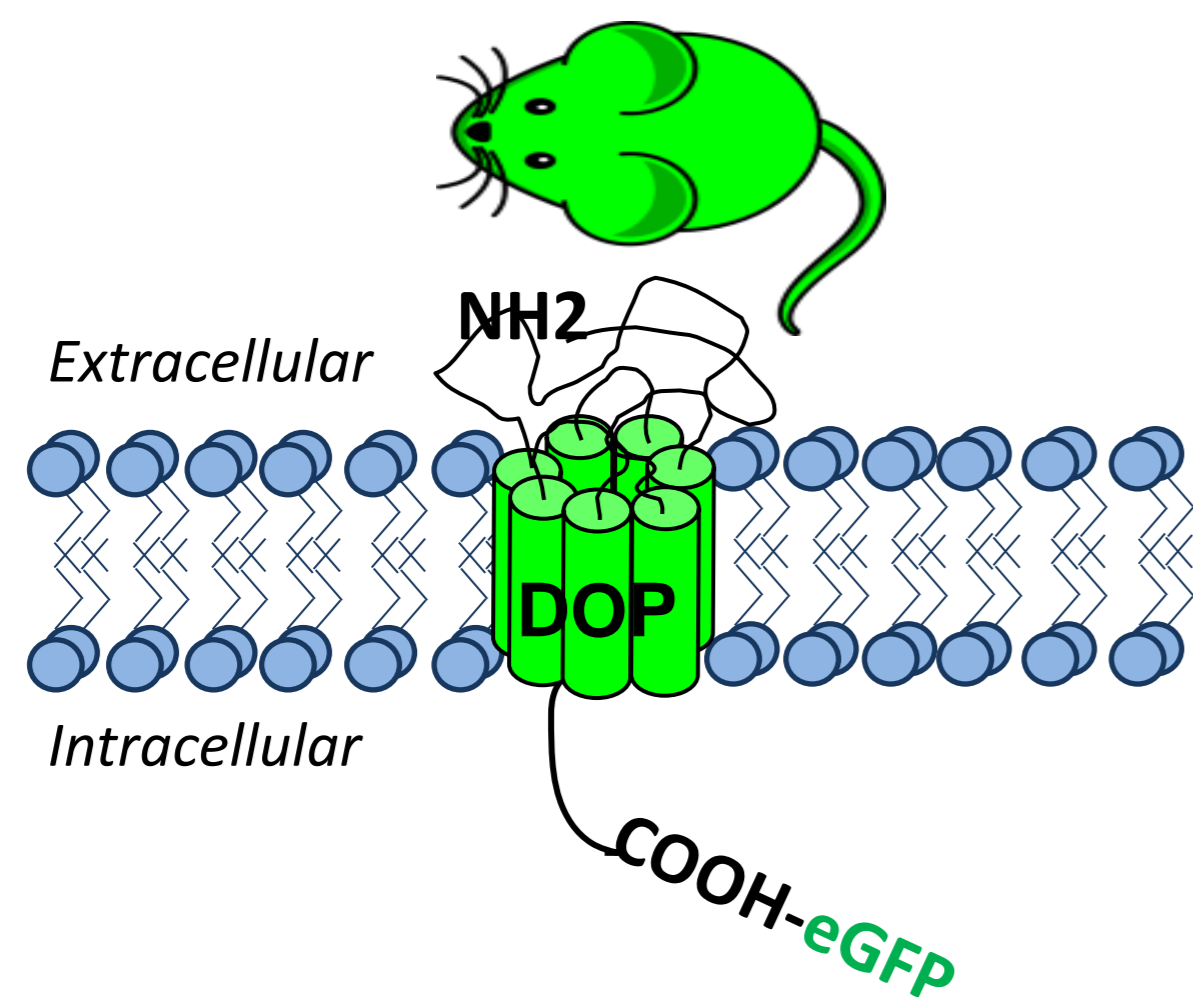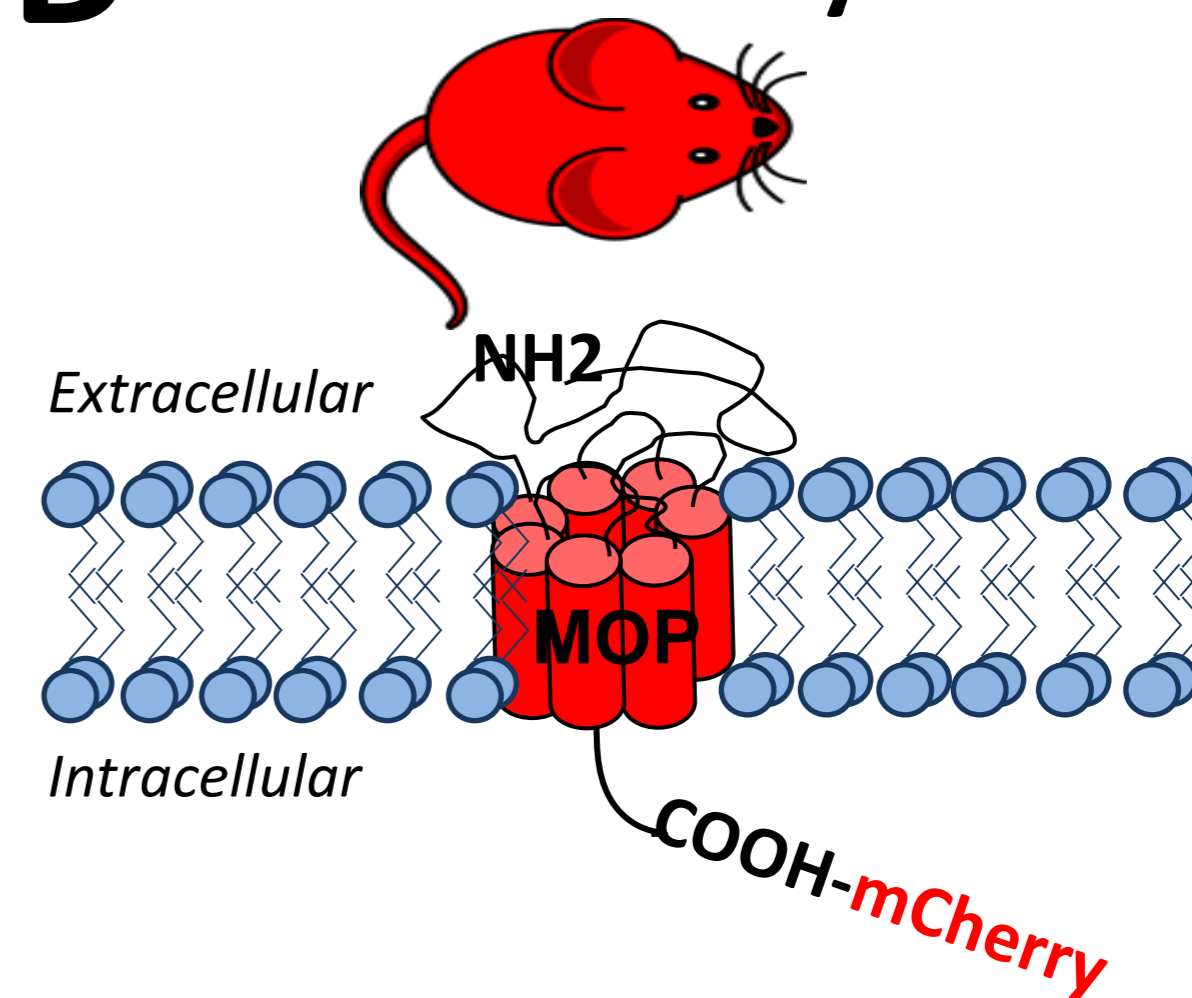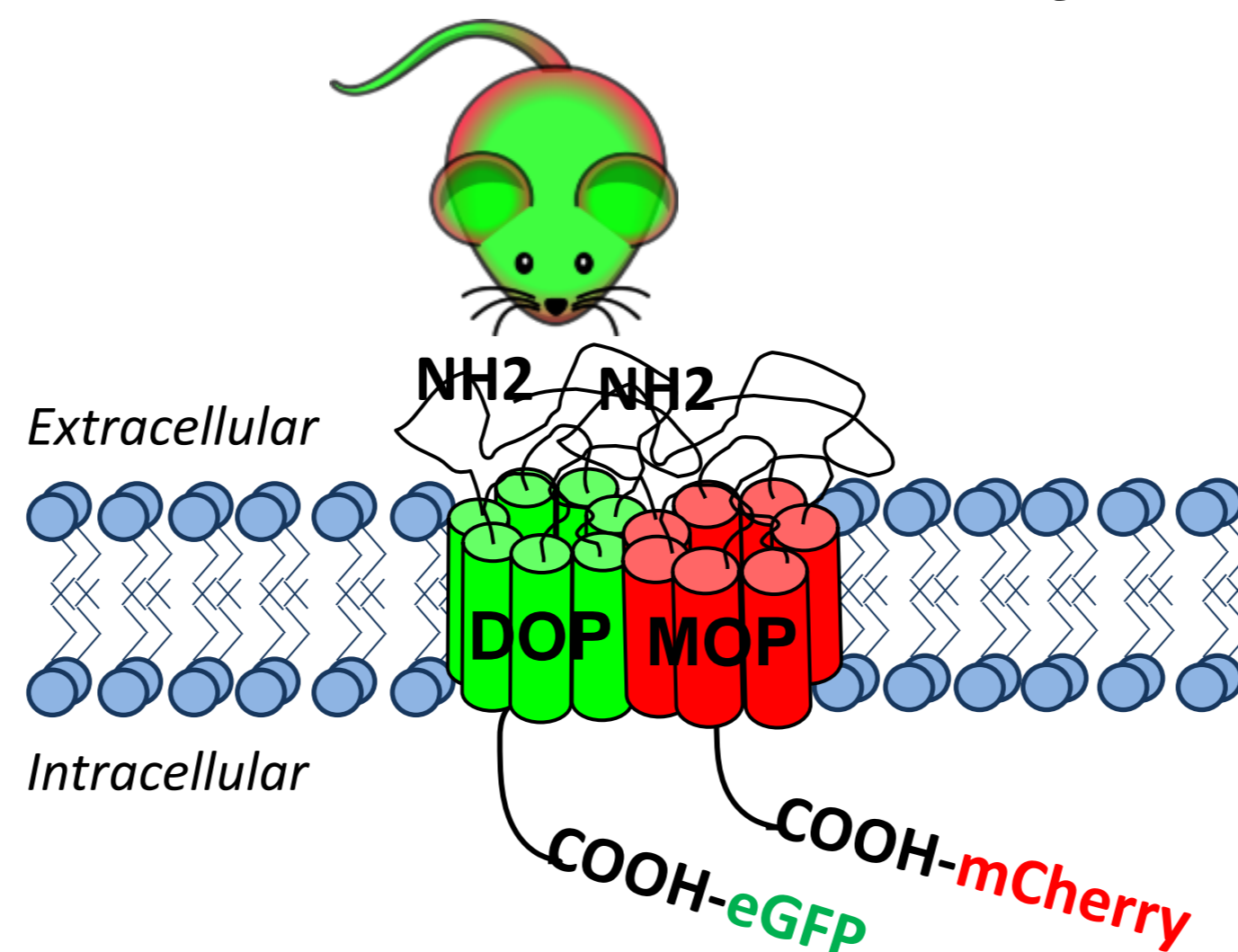
446   or after treatment during 60 minutes with the MOP-DOP agonist CYM51010 400nM. Scale

447   bar: 5µm. **B)** Image quantification with ICY software illustrating each receptor distribution.

448   In basal conditions, MOP and DOP densities are significantly higher in the plasma

449   membrane compared to cytoplasm. Mann Witney test, *p-value <0.05. CYM51010 treatment

450   for 60 minutes led to changes in receptor subcellular distribution with no more statistical

451   difference in receptor densities between the plasma membrane and cytoplasm (Mann Witney

452   test, p-value > 0.05). **C)** Changes in receptors distribution. Plasma membrane to cytoplasm

453   ratio of MOP or DOP spots densities in basal conditions or after with 400nM CYM51010 for

454   60 minutes reflects receptor redistribution. Mann Witney test, ****p-value <0.001; **** p-value

455   <0.0001. **D)** Quantification of MOP-DOP co-localisation upon agonist activation with 400nM

456   CYM51010 for 60 minutes reveals MOP-DOP co-internalisation. Two-way ANOVA with

457   repeated measures, post-hoc Sidak's test. *p-value <0.05 for basal cytoplasm *vs* CYM51010

458   cytoplasm; **p-value <0.01 for basal membrane *vs* CYM51010 membrane. ### p-value <0.001

459   for basal membrane *vs* basal cytoplasm; NS: p-value >0.05 for CYM51010 membrane vs

460   CYM51010 cytoplasm.

461

A
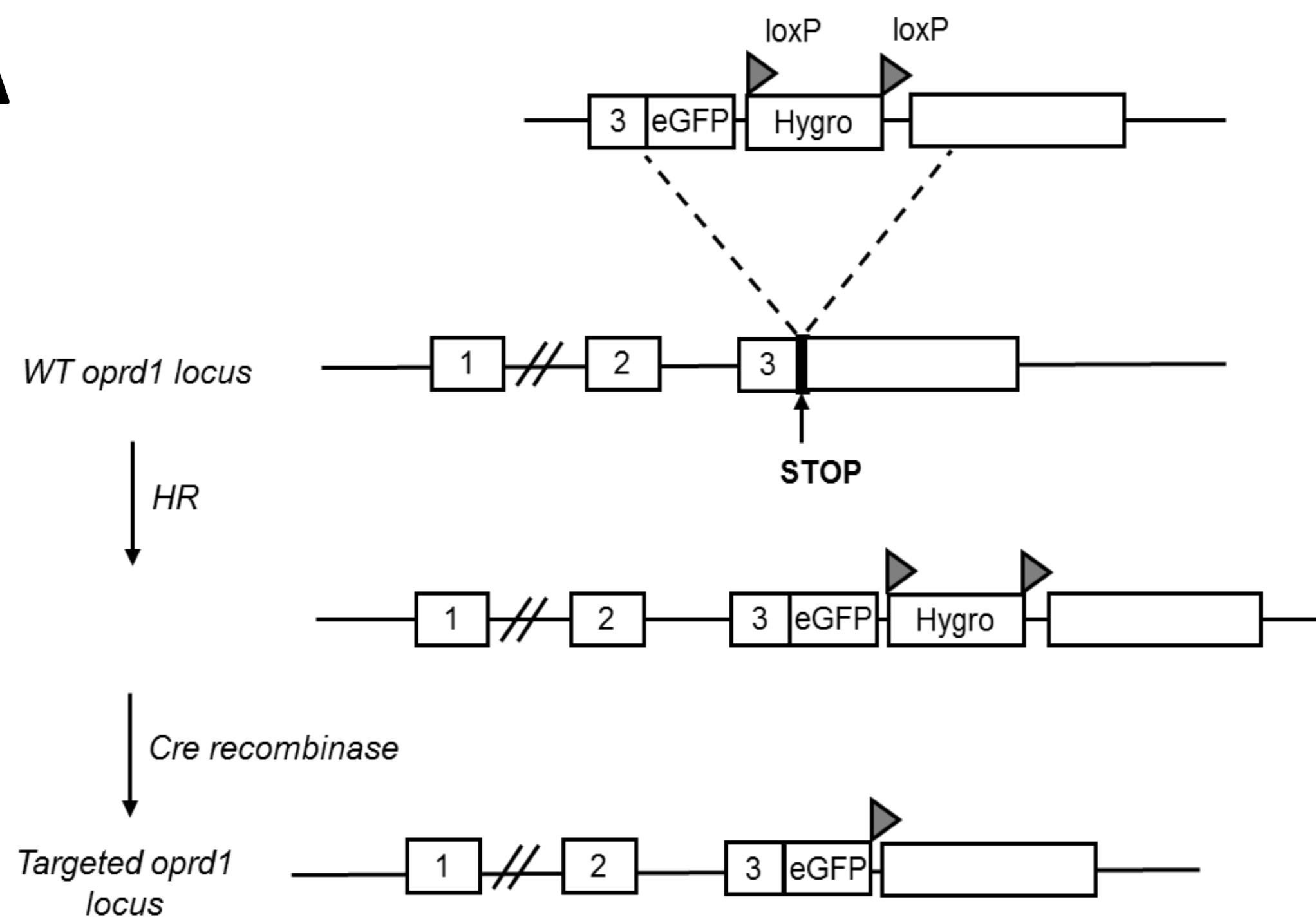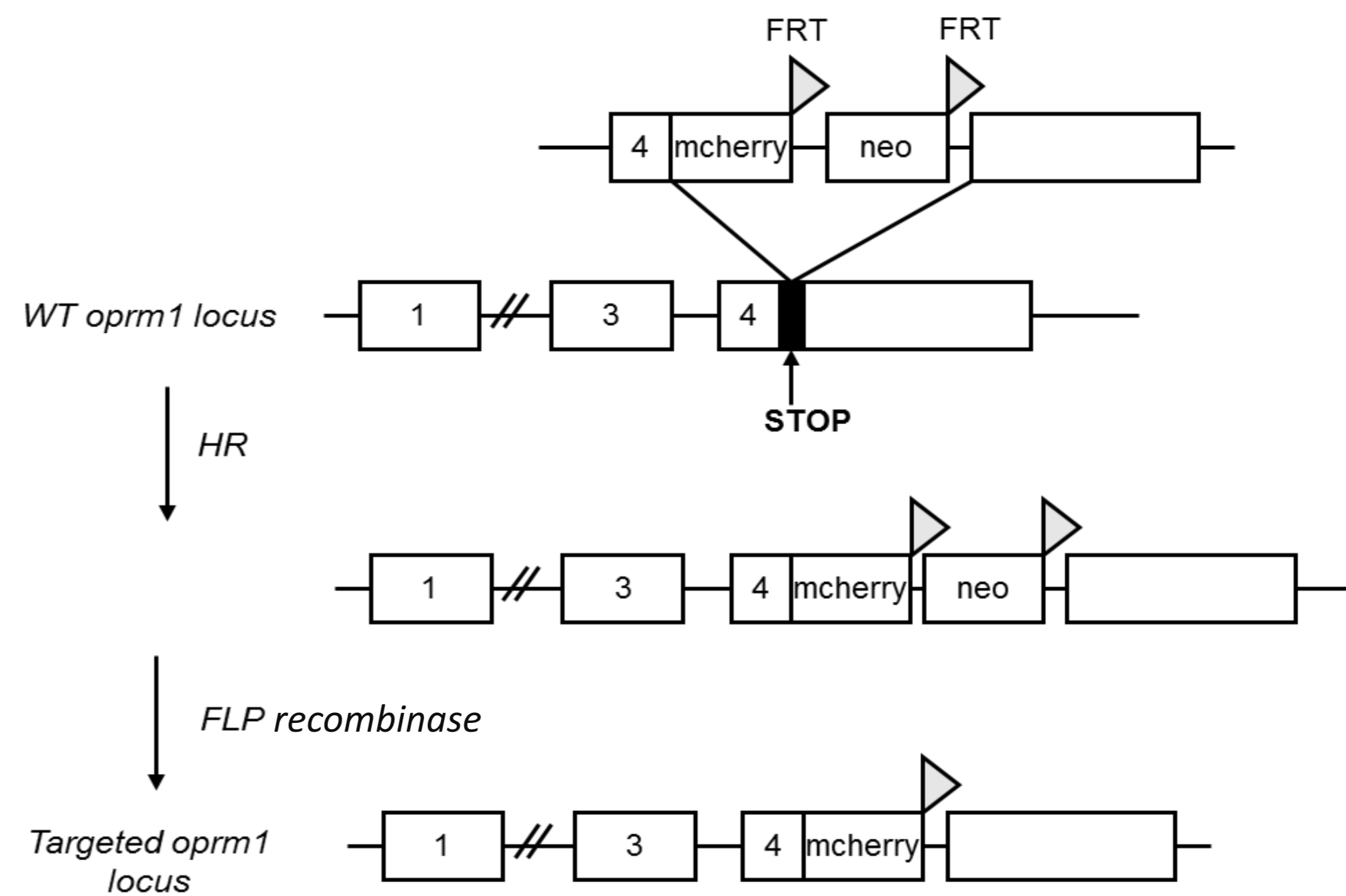
loxP loxP

3 | eGFP | Hygro

WT oprd1 locus

1 | 2 | 3

STOP

HR

1 | 2 | 3 | eGFP | Hygro

Cre recombinase

Targeted oprd1 locus

1 | 2 | 3 | eGFP

B

FRT FRT

4 | mcherry | neo

WT oprm1 locus

1 | 3 | 4

STOP

HR

1 | 3 | 4 | mcherry | neo

FLP recombinase

Targeted oprm1 locus

1 | 3 | 4 | mcherry

C DOP-eGFP/

NH2

Extracellular

DOP

Intracellular

COOH-eGFP

D MOP-mCherry

NH2

Extracellular

MOP

Intracellular
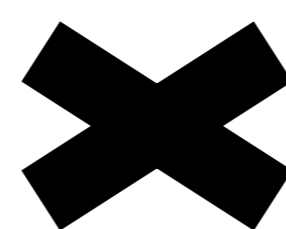
COOH-mCherry

E DOP-eGFP/MOP-mCherry

NH2 NH2

Extracellular

DOP MOP

Intracellular

COOH-eGFP COOH-mCherry